

# Realization of a monolithic high-reflectivity cavity mirror from a single silicon crystal

Frank Brückner,<sup>1</sup> Daniel Friedrich,<sup>2</sup> Tina Clausnitzer,<sup>1</sup> Michael Britzger,<sup>2</sup> Oliver Burmeister,<sup>2</sup>  
Karsten Danzmann,<sup>2</sup> Ernst-Bernhard Kley,<sup>1</sup> Andreas Tünnermann,<sup>1</sup> and Roman Schnabel<sup>2</sup>

<sup>1</sup>*Institute of Applied Physics, Friedrich-Schiller-University Jena, Max-Wien-Platz 1, 07743 Jena, Germany*

<sup>2</sup>*Albert-Einstein-Institute, Max-Planck-Institute for Gravitational Physics  
and Leibniz University Hannover, Callinstr. 38, 30167 Hannover, Germany*

(Dated: July 7, 2009)

Cavity mirrors for laser radiation are essential as heavy test masses of space-time for the new field of gravitational wave astronomy<sup>1,2</sup>, as mechanical oscillators for targeting the quantum regime of macroscopic mechanical devices<sup>3-5</sup>, and for ultra-high-precision optical clocks designed for researching the nature of fundamental constants<sup>6-9</sup>. Current limitations in all fields are set by the joint problem of lacking appropriate cavity mirror qualities. The currently used dielectrically coated mirrors can show very high reflectivities but always at the cost of a reduced mechanical quality, i.e. at the cost of a thermal noise increase. Here we report on the first experimental realization of a high reflectivity surface mirror that solely consists of a single silicon crystal. Since no material was added to the crystal, the problem of ‘coating’ thermal noise is avoided. Our mirror is based on a recently proposed surface nanostructure<sup>10</sup> that creates a resonant surface waveguide, and achieved a reflectivity of  $(99.79 \pm 0.01) \%$  and a cavity finesse of 2784 at a wavelength of  $1.55 \mu\text{m}$ , in full agreement with a rigorous model. Perfect reflectivities of 100 % are theoretically possible, and we anticipate that our achievement will open the avenue to new generations of a variety of experiments targeting fundamental questions of physics.

The purpose of cavity mirrors is to repeatedly retro-reflect laser light such that it constructively interferes with the stored cavity field yielding maximum field amplitudes and providing an output field of highest phase stability. In order to do so cavity mirrors need high reflectivities and a geometrically well-defined surface profile. If the mirror surface shows statistical fluctuations, for example driven by Brownian motion of the mirror’s molecules, the phase fronts of subsequently reflected waves are slightly different and cannot perfectly interfere constructively, which results in a reduced cavity built-up and, most severely, in changes of the phase of the output laser beam. Motions of mirror surfaces, driven by thermal energy, are known as *thermal noise* and currently a major limiting factor in many research fields targeting fundamental questions of nature as mentioned above.

The best approach for a thermal noise reduction is to employ crystalline materials with high mechanical quality factors (Q-factors) and low absorption of the laser light, at cryogenic temperatures. Within the past years silicon was found to be a promising candidate with an absorption of probably less than  $10^{-8} \text{ cm}^{-1}$  at a 1550 nm wavelength<sup>11</sup> and Q-factors of  $10^9$  at cryogenic temperatures<sup>12</sup>. Unfortunately, the reflectivity of silicon for laser light under normal incidence is only of the order of 30 %, hence a pure polished silicon surface can not be

used as a mirror in a high-finesse cavity. In order to achieve high reflectivities dielectric multilayer coatings on the substrate’s surface are currently employed, and reflectivities of up to 99.9998 % have been demonstrated<sup>13</sup>. However, recent theoretical and experimental research revealed that these coatings result in a significant reduction of Q-factors and, thus, a rapidly increased thermal noise level<sup>14-17</sup>. Thus, besides optimizing multilayer stacks<sup>18,19</sup>, a coating-free (i.e. monolithic) mirror concept is of enormous interest. Previous published approaches<sup>20,21</sup> are based on total internal reflection which is connected with additional optical paths inside a substrate giving rise to absorption and increased thermorefractive noise resulting from a temperature dependent index of refraction.

This work experimentally demonstrates for the first time a monolithic surface mirror (see Fig. 1a), i.e. a single piece of mono-crystalline silicon, with a reflectivity high enough to form a laser cavity with a finesse of almost 3000. The achieved high reflectivity does not rely on multiple interference (at coating layers) but on resonant coupling to a guided optical mode of a surface nanostructure<sup>22-24</sup>. Since no material is added to the silicon substrate, the coating thermal noise as found in Ref.<sup>14,15</sup> is avoided. A recent experiment showed that a surface periodic nanostructure did not reduce the substrate’s high Q-factor of the order  $10^8$ , Ref.<sup>16</sup>.

In Figs. 1b-e we plot the evolution from previous non-monolithic to the monolithic guided-mode resonant waveguide grating mirror and we use a simplified ray picture<sup>23</sup> in order to explain how it achieves a high reflectivity close to unity. The mirror architecture in Fig. 1b uses a second material coated on the substrate’s surface, and was initially proposed for narrowband optical filters and switching applications in the mid 1980s. It comprises a periodically corrugated high-refractive index layer attached to a low-refractive index substrate. In order to allow for resonant reflection under normal incidence, the corrugation period must fulfill the following parameter inequalities, which can be derived from the well-known grating equation<sup>25</sup>:

$$d < \lambda \quad (\text{to permit only zeroth order in air}), \quad (1)$$

$$\lambda/n_H < d \quad (\text{first orders in high-index layer}), \quad (2)$$

$$d < \lambda/n_L \quad (\text{only zeroth order in substrate}), \quad (3)$$

where  $d$  is the grating period,  $\lambda$  is the light’s vacuum wavelength and  $n_H$  and  $n_L$  are the higher and lower refractive indices, respectively. In our simplified ray picture, the first diffraction orders (-1T, +1T) within the high-index layer can experience total internal reflection (at the interface to the low-

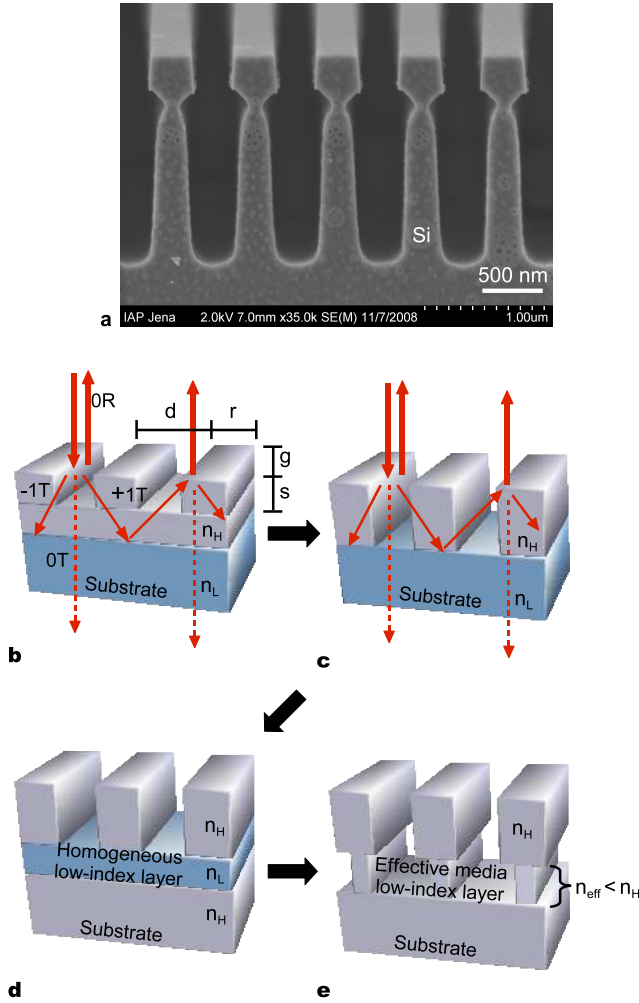


**FIG. 1: Monolithic mirror from a nanostructured single silicon crystal.** **a**, SEM (scanning electron microscope) cross-sectional view of a 700 nm period T-shaped grating in a silicon bulk substrate that forms the monolithic cavity mirror's surface, efficiently reflecting normally incident light with a wavelength of 1.55  $\mu\text{m}$ . **b**, Conventional resonant waveguide grating with a high-index layer corrugated at its surface on top of a low-index substrate. **c**, Stand-alone high-index grating ridges corresponding to a zero waveguide layer thickness ( $s = 0$  nm). **d**, Reduction of the low-index substrate to a thin layer. **e**, For the monolithic implementation of the element in **d**, the homogeneous low-index layer is replaced by an effective media low-index layer to advance the resonant device to a monolithic reflector (light rays have been omitted for clarity).

index substrate) and, thus, can excite resonant waveguide modes propagating along the corrugated high-index layer. In turn, a certain fraction of the light inside the waveguide is coupled out again via the grating to both, the transmitted and reflected zeroth order (0T, 0R). If the grating period  $d$ , the groove depth  $g$ , the grating fill factor  $f$  (ratio between ridge width  $r$  and grating period  $d$ ), and the high-index layer thickness  $s$  with respect to the refractive index values of the involved materials are designed properly, all transmitted light can be prompted to interfere destructively, corresponding to

a reflectivity of 100%. Fig. 1c illustrates that the same principle even works if the homogeneous part of the waveguide layer has zero thickness as proposed and realized in Ref.<sup>25,26</sup>. The low-index substrate which is necessary for total internal reflection can be reduced to a layer<sup>24</sup>, see Fig. 1d. This layer has to have a certain minimum thickness, for which evanescent transmission of the higher orders is still low. Although these approaches reduce the thick dielectric multilayer stack of conventional mirrors to a thin waveguide layer, at least one additional material has to be added still resulting in an increased mechanical loss.

Eventually, as shown in Fig. 1e, we proposed to replace the remaining low-index layer by an *effective* low-index layer<sup>10</sup>. This grating layer exhibits the same period but has a lower fill factor (LFF) than the structure on top, and has an effective index  $n_{\text{eff}} < n_H$ . Since the high fill factor (HFF) grating on top generates higher diffraction orders, referring to Ineq. (2), the realization of the LFF grating as an effective medium is not obvious<sup>27</sup>. Only if the fill factor is sufficiently low, no higher diffraction orders are allowed to propagate as required, according to Ineq. (3). We note that the electromagnetic field inside this T-shaped periodic structure can be expressed by discrete grating modes<sup>28</sup>. These modes correspond to the diffraction orders within a conventional resonant waveguide grating. Similar to the higher diffraction orders within a conventional waveguiding layer, the resonant excitation of these modes can result in a destructive interference of all light transmitted to the LFF grating. Thus, the monolithic T-shaped grating, as depicted in Fig. 1e, can be optimized to create 100% reflectivity.

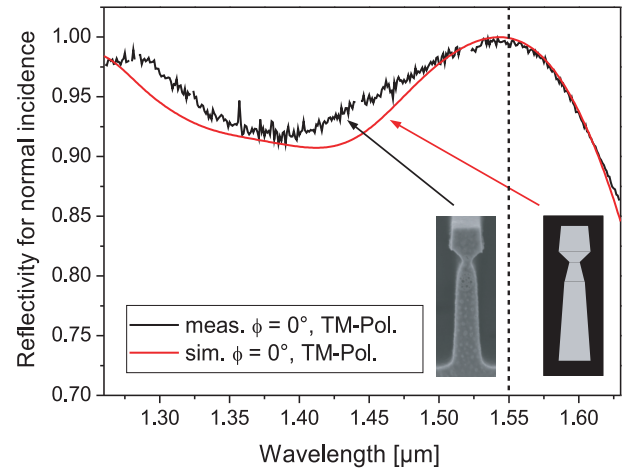


**FIG. 2: Spectral reflectivity.** Measured spectral reflectivity of the grating from Fig. 1a for normal incidence ( $\phi = 0 \pm 1^\circ$ ) (black curve) and rigorously simulated spectral reflectivity for a grating profile approximating the real shape by a trapezoidal fragmentation (red curve).

The design of our monolithic silicon mirror architecture was developed by means of a rigorous simulation<sup>29</sup> with the goal of obtaining 100% reflectivity under normal incidence of TM-polarized light (electric field vector oscillating perpendicular to the grating ridges) with a wavelength of 1550 nm. An

additional goal was to achieve large parameter tolerances for the fabrication process and resulted in a grating with a 700 nm period<sup>10</sup>.

Fig. 1a depicts an SEM (scanning electron microscope) cross-sectional view on the mirror surface that has been characterized within this work. As expected, the shape of the grating ridges was not strictly rectangular, but it was within the parameter tolerances that predict high reflectivity<sup>10</sup> (for details of the fabrication see the method box).

The first measurement of the mirror's reflectivity was performed under normal incidence ( $0 \pm 1^\circ$ ) and employed a fiber-coupled tunable diode laser. The measured data is shown in Fig. 2 (black curve) and reveals a reflectivity of higher than 91.5 % for a rather broad spectral range from approximately 1.21  $\mu\text{m}$  to 1.61  $\mu\text{m}$ . The peak reflectivity is located close to the design wavelength of 1.55  $\mu\text{m}$  with a value of almost 100%, where a measurement error of  $\pm 0.3\%$  needs to be taken into account. The red curve in Fig. 2 represents a rigorously simulated spectral response for a grating profile that has been formed by a trapezoidal fragmentation in order to approximate the real shape (indicated by the sketch on the bottom right hand side of Fig. 2).

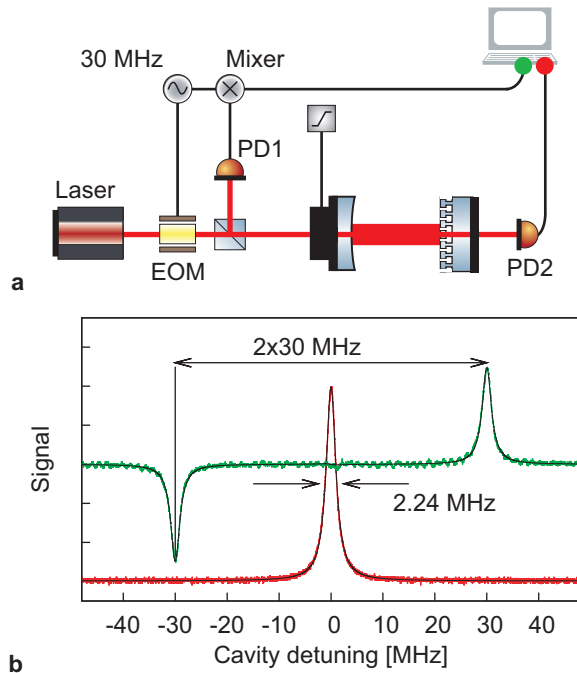


FIG. 3: **High-finesse cavity setup with monolithic end mirror.** **a**, Experimental setup for the characterization of the waveguide grating as a cavity end mirror. Electro-optical-modulator (EOM), photodiode (PD). **b**, Scan over one cavity resonance (airy) peak (red line) with a linewidth of 2.24 MHz measured in transmission (PD2), corresponding to a cavity finesse of 2784 and a power reflectivity of the monolithic mirror of 99.79 %. The cavity detuning was calibrated via the demodulated signal (frequency markers at  $\pm 30$  MHz, green line) in reflection of the cavity (PD1) that was generated with the PDH technique. Fitted theoretical lines are in black.

In order to demonstrate the high optical quality of our monolithic mirror we incorporated it as the end mirror in a

standing-wave Fabry-Perot resonator, see Fig. 3a. A conventional high quality multilayer coated mirror served as the coupling mirror with a measured power transmittivity of  $\tau_1^2 = (200 \pm 20)$  ppm. Note that the monolithic mirror substrate had an unpolished rear surface and could not be used as the coupling mirror. By measuring the cavity's finesse  $F$ , this setup also enabled us to precisely determine the mirror's reflectivity under an angle of incidence of precisely zero degree at a wavelength of 1550 nm. The product of the amplitude reflectivities  $\rho_{12} = \rho_1 \rho_2$  of coupling mirror and end mirror, respectively, can be calculated from a measured finesse as follows

$$\rho_{12} = \rho_1 \rho_2 = 2 - \cos \frac{\pi}{F} - \sqrt{\left(\cos \frac{\pi}{F} - 2\right)^2 - 1}. \quad (4)$$

The finesse  $F$  is defined as the ratio of free spectral range (FSR)  $\nu_{\text{FSR}}$  and cavity linewidth  $\Delta\nu$  (full width at half maximum). The FSR was  $\nu_{\text{FSR}} = c/(2L) = (6.246 \pm 0.13)$  GHz with  $c$  the speed of light and  $L = (24 \pm 0.5)$  mm the distance between both mirrors. The linewidth was determined to  $\Delta\nu = (2.24 \pm 0.07)$  kHz (see Fig. 3b). Hence, the finesse was found to be  $F = 2784 \pm 100$ , which corresponds to a waveguide grating power reflectivity of  $\rho_2^2 = (99.7945 \pm 0.0086)\%$ , referring to Eq. (4) (for further information see the method box and supplementary information).

The optical reflectivity measured here is, to the best of our knowledge, the highest resonant reflection ever realized. The measured reflectivity of slightly below unity is in very good agreement with the experimental data as well as with the simulated fit in Fig. 2 that predict a reflectivity maximum for a slightly shorter wavelength of about 1.543  $\mu\text{m}$ . However, this could not be verified in our cavity setup since the laser source was not tunable into this wavelength regime.

The high cavity finesse of 2784, as demonstrated here, already reaches the regime of finesse values used in gravitational wave detectors. For example, the Advanced LIGO Fabry-Perot arm cavities are being designed for a finesse of a few hundred. Our demonstrated monolithic mirror quality may also be already sufficient to provide an impact towards reaching the quantum regime of micro-mechanical oscillators. In Ref.<sup>3</sup> optical cooling of a micro-mechanical oscillator down to 135 mK was achieved with a finesse of only 200. Our demonstrated cavity linewidth of 2.24 MHz is significantly smaller than many typical fundamental oscillator frequencies and the so-called good cavity regime can be reached<sup>4</sup>. Note that the cavity linewidth can be further reduced by increasing the cavity length. For applications in reference cavities and optical clocks<sup>7,8</sup> the reflectivities should be further increased beyond the value demonstrated here, however, we expect that indeed considerable improvements towards a perfect reflectivity are possible with improved electron beam lithography and etching technologies. Having demonstrated the first monolithic surface mirror ever, our future work now aims for the realization of even higher reflectivities and for an in situ experimental confirmation that the thermal noise of our mirror concept is for fundamental reasons much lower than any other high-reflectivity mirror concept.

## METHODS

**Lithography and dry etching.** For fabrication, a standard silicon wafer with 100 mm in diameter was thermally oxidized with a 1  $\mu\text{m}$  silica layer and coated with a 80 nm chromium layer, both serving as the mask during the silicon etching process. After spin-coating an electron beam sensitive (chemically amplified) resist on top, the 700 nm period grating was defined by means of electron beam lithography for an area of (7.5 x 13)  $\text{mm}^2$ , aiming at a grating fill factor of 0.56<sup>10</sup>. The developed binary resist profile was then transferred into the chromium layer and subsequently into the oxidized silica layer as well as the silicon bulk substrate by utilizing an anisotropic (i.e. binary) ICP (Inductively-Coupled-Plasma) dry etching process. Here, the etching time was adjusted to match the desired groove depth of the upper silicon grating of about 350 nm. The vertical grating groove side walls were then covered with a thin chromium layer by coating the whole device under an oblique angle. By using this technique, the groove side walls were protected from further ICP etching while the groove bottom remained accessible. A second, but this time isotropic (i.e. polydirectional), ICP etching process enabled the undercut of the upper grating to generate the low fill factor grating beneath. Here, a well-balanced ratio between horizontal and vertical etching rate played a decisive role to supply a sufficiently low grating fill factor (< 0.3) as well as a minimum groove depth of the lower grating of about

500 nm simultaneously<sup>10</sup>. Finally, the etching mask materials (silica, chromium, and resist) were removed by means of wet chemical etching baring the mono-crystalline silicon surface structure.

### Cavity-based measurement of the mirror's reflectivity.

In order to obtain the linewidth of the linear Fabry-Perot resonator we used a calibrated tuning of the cavity length around an airy peak. The calibration was done via frequency markers at  $\pm 30$  MHz around an airy peak using the Pound-Drever-Hall (PDH) technique<sup>30</sup>, see Fig. 3a,b. For this purpose, a phase modulation was imprinted on the light by an electro-optical modulator (EOM). The detected signal in reflection (PD1) was then electronically demodulated by a local oscillator. We investigated 25 beam positions on the grating over an area of 4  $\text{mm}^2$  with a beam size radius of  $\approx 50 \mu\text{m}$ . For each position, we did 12 measurements of the linewidth, which resulted in an averaged value of the power reflectivity of  $\bar{\rho}_2^2 = (99.7682 \pm 0.0095)\%$  for the overall area. The position of highest finesse showed  $F = (2784 \pm 100)$ , which corresponds to a power reflectivity of  $\rho_2^2 = (99.7945 \pm 0.0086)\%$  and would allow a maximum finesse of  $\approx 3050$ , if we assume the coupling mirror to exhibit a 100% reflectivity. Due to the unpolished back side of the substrate we could only set a lower limit on the transmission by means of power measurements of  $\tau_2^2 \geq (230 \pm 20)$  ppm and, hence, an upper limit on optical losses due to absorption and scattering of  $(1820 \pm 110)$  ppm.

- 
- <sup>1</sup> Aufmuth, P. & Danzmann, K. Gravitational wave detectors. *New J. Phys.* **7**, 202 (2005).
- <sup>2</sup> Smith, J.R. (for the LIGO Scientific Collaboration) The path to the enhanced and advanced LIGO gravitational-wave detectors. *Class. Quantum Grav.* **26**, 114013 (2009).
- <sup>3</sup> Kleckner, D. & Bouwmeester, D. Sub-kelvin optical cooling of a micromechanical resonator. *Nature* **444**, 75-78 (2006).
- <sup>4</sup> Schliesser, A., Arcizet, O., Riviere, R., Anetsberger, G., & Kippenberg, T. J. Resolved-sideband cooling and position measurement of a micromechanical oscillator close to the Heisenberg uncertainty limit. *Nature Physics* **5**, 509-514 (2009).
- <sup>5</sup> Müller-Ebhardt, H., Rehbein, H., Schnabel, R., Danzmann, K. & Chen, Y. Entanglement of Macroscopic Test Masses and the Standard Quantum Limit in Laser Interferometry. *Phys. Rev. Lett.* **100**, 013601 (2008).
- <sup>6</sup> Udem, Th., Holzwarth, R. & Hänsch, T. W. Optical frequency metrology. *Nature* **416**, 233-237 (2002).
- <sup>7</sup> Young, B. C., Cruz, F. C., Itano, W. M. & Bergquist, J. C. Visible Lasers with Subhertz Linewidths. *Phys. Rev. Lett.* **82**, 3799-3802 (1999).
- <sup>8</sup> Braxmaier, C., Pradl, O., Müller, H., Peters, A. & Mlynek, J. Proposed test of the time independence of the fundamental constants  $\alpha$  and  $m_e/m_p$  using monolithic resonators. *Phys. Rev. D* **64**, 042001 (2001).
- <sup>9</sup> Numata, K., Kemery, A. & Camp, J. Thermal-Noise Limit in the Frequency Stabilization of Lasers with Rigid Cavities. *Phys. Rev. Lett.* **93**, 250602 (2004).
- <sup>10</sup> Brückner, F., Clausnitzer, T., Burmeister, O., Friedrich, D., Kley, E.-B., Danzmann, K., Tünnermann, A. & Schnabel R. Monolithic dielectric surfaces as new low-loss light-matter interfaces. *Opt. Lett.* **33**, 264-266 (2008).
- <sup>11</sup> Green, M. A. & Keevers, M. J. Optical properties of intrinsic silicon at 300 K. *Prog. Photovoltaic Res. Appl.*, **3**, 189-192 (1995).
- <sup>12</sup> McGuigan, D. F., Lam, C. C., Gram, R. Q., Hoffman, A. W., Douglass, D. H. & Gutche, H. W. Measurements of the Mechanical Q of Single-Crystal Silicon at Low Temperatures. *J. Low Temp. Phys.* **30**, 621-629 (1978).
- <sup>13</sup> Rempe, G., Thompson, R. J., Kimble, H. J. & Lalezari, R. Measurement of ultralow losses in an optical interferometer. *Opt. Lett.* **17**, 363-365 (1992).
- <sup>14</sup> Harry, G. M., Gretarsson, A. M., Saulson, P. R., Kittelberger, S. E., Penn, S. D., Startin, W. J., Rowan, S., Fejer, M. M., Crooks, D. R. M., Cagnoli, G., Hough, J. & Nakagawa, N. Thermal noise in interferometric gravitational wave detectors due to dielectric optical coatings. *Class. Quantum Grav.* **19**, 897-917 (2002).
- <sup>15</sup> Levin, Y. Internal thermal noise in the LIGO test masses: A direct approach. *Phys. Rev. D* **57**, 659-663 (1998).
- <sup>16</sup> Nawrodt, R., Zimmer, A., Koettig, T., Clausnitzer, T., Bunkowski, A., Kley, E.-B., Schnabel, R., Danzmann, K., Nietzsche, S., Vodel, W., Tünnermann, A. & Seidel, P. Mechanical Q-factor measurements on a test mass with a structured surface. *New J. Phys.* **9**, 225 (2007).
- <sup>17</sup> Black, E. D., Villar, A., Barbary, K., Bushmaker, A., Heefner, J., Kawamura, S., Kawazoe, F., Matone, L., Meidt, S., Rao, S. R., Schulz, K., Zhang, M. & Libbrecht, K. G. Direct observation of broadband coating thermal noise in a suspended interferometer. *Phys. Lett. A* **328**, 1-5 (2004).
- <sup>18</sup> Agresti, J., Castaldi, G., DeSalvo, R., Galdi, V., Pierro, V., Pinto, I. M. Optimized multilayer dielectric mirror coatings for gravitational wave interferometers. *Proc. SPIE* **6286**, 628608 (2006).

- <sup>19</sup> Harry, G. M., Armandula, H., Black, E., Crooks, D. R. M., Cagnoli, G., Hough, J., Murray, P., Reid, S., Rowan, S., Sneddon, P., Fejer, M. M., Route, R. & Penn, S. D. Thermal noise from optical coatings in gravitational wave detectors. *Appl. Opt.* **45**, 1569-1574 (2006).
- <sup>20</sup> Cella, G. & Giazotto, A. Coatingless, tunable finesse interferometer for gravitational wave detection. *Phys. Rev D.* **74**, 042001 (2006).
- <sup>21</sup> Goßler, S., Cumpston, J., McKenzie, K., Mow-Lowry, C. M., Gray, M. B. & McClelland, D. E. Coating-free mirrors for high precision interferometric experiments. *Phys. Rev A.* **76**, 053810 (2007).
- <sup>22</sup> Golubenko, G. A., Svakhin, A. S., Sychugov, V. A. & Tishchenko, A. V. Total reflection of light from a corrugated surface of a dielectric waveguide. *Sov. J. Quantum Electron.* **15**, 886-887 (1985).
- <sup>23</sup> Sharon, A., Rosenblatt, D. & Friesem, A. A. Resonant grating-waveguide structures for visible and near-infrared radiation. *J. Opt. Soc. Am. A* **14**, 2985-2993 (1997).
- <sup>24</sup> Mateus, C. F. R., Huang, M. C. Y., Chen, L., Chang-Hasnain, C. J. & Suzuki, Y. Broad-Band Mirror (1.12 - 1.62  $\mu\text{m}$ ) Using a Subwavelength Grating. *IEEE Phot. Techn. Lett.* **16**, 1676-1678 (2004).
- <sup>25</sup> Bunkowski, A., Burmeister, O., Friedrich, D., Danzmann, K. & Schnabel, R. High reflectivity grating waveguide coatings for 1064 nm. *Class. Quantum Grav.* **23**, 7297-7303 (2006).
- <sup>26</sup> Brückner, F., Friedrich, D., Clausnitzer, T., Burmeister, O., Britzger, M., Kley, E.-B., Danzmann, K., Tünnermann, A. & Schnabel R. Demonstration of a cavity coupler based on a resonant waveguide grating. *Opt. Express* **17**, 163-169 (2009).
- <sup>27</sup> Lalanne, P. & Lemerrier-Lalanne, D. On the effective medium theory of subwavelength periodic structures. *J. Mod. Opt.* **43**, 2063-2085 (1996).
- <sup>28</sup> Clausnitzer, T., Kämpfe, T., Kley, E.-B., Tünnermann, A., Peschel, U., Tishchenko, A. V. & Parriaux, O. An intelligible explanation of highly-efficient diffraction in deep dielectric rectangular transmission gratings. *Opt. Express* **13**, 10448-10456 (2005).
- <sup>29</sup> Moharam, M. G. & Gaylord, T. K. Rigorous coupled-wave analysis of planar-grating diffraction. *J. Opt. Soc. Am.* **71**, 811-818 (1981).
- <sup>30</sup> Drever, R. W. P., Hall, J. L., Kowalski, F. V., Hough, J., Ford, G. M., Munley, A. J. & Ward, H. Laser phase and frequency stabilization using an optical resonator. *Appl. Phys. B.* **31**, 97-105 (1983).

### Acknowledgements

We acknowledge financial support from the Deutsche Forschungsgemeinschaft (DFG) within the Collaborativ

Research centre TR7. We also acknowledge the centre of excellence QUEST for the allocation of the 1.55  $\mu\text{m}$  laser source.

### Competing Interests

The authors declare that they have no competing financial interests.

### Correspondence

Correspondence and requests for materials should be addressed to R. Schnabel (email: roman.schnabel@aei.mpg.de).

### Supplementary Information

#### Error propagation regarding the mirror's reflectivity.

For the experimental deduction of the reflectivity of our monolithic mirror, the PDH-signal as well as the airy peak were fitted in order to obtain a calibration for the detuning of the cavity and subsequently the linewidth. The experimental error for the marker frequency is caused by uncertainties in adjusting the demodulation phase and locating their peak position. Concerning the linewidth we took the standard deviation of the mean value ( $g\sigma/\sqrt{n}$ , with  $n$  the number of measurements and a confidence factor of  $g = 2.2$ ). The FSR was obtained from a length measurement. Since the transmittivity of the coupling mirror was measured via power measurements we assumed an error of 10 %. We did an error propagation for each value according to  $\rho_2^2 = (\rho_{12}/\rho_1)^2$ . The results are listed in Tab. I. Since all errors are independent of each other, they sum up to a total rms-error for the waveguide grating power reflectivity.

TABLE I: Error propagation

Quantity	Error	Projected error for $\rho_2^2$
Marker frequency $f_m = \pm 30$ MHz	$\pm 0.5$ %	$\pm 11$ ppm
Linewidth $\Delta\nu = 2.24$ MHz	$\pm 3$ %	$\pm 68$ ppm
Cavity length $L = 24$ mm	$\pm 0.5$ mm	$\pm 47$ ppm
Coupling mirror $\tau_1^2 = 200$ ppm	$\pm 10$ %	$\pm 20$ ppm
total rms error		$\pm 86$ ppm